Supporting information for:

Photothermic regulation of gene expression triggered by laser-induced carbon nanohorns

Eijiro Miyako[a,1], Tomonori Deguchi[b], Yoshihiro Nakajima[c], Masako Yudasaka[d], Yoshihisa Hagihara[a], Masanori Horie[a,2], Mototada Shichiri[a], Yuriko Higuchi[e], Fumiyoshi Yamashita[e], Mitsuru Hashida[e], Yasushi Shigeri[e], Yasukazu Yoshida[a,c] and Sumio Iijima[d,f,g,1]

[a]Health Research Institute (HRI), National Institute of Advanced Industrial Science and Technology (AIST), 1-8-31 Midorigaoka, Ikeda, Osaka 563-8577, Japan; [b]HRI, AIST, 3-11-46 Nakouji, Amagasaki, Hyogo 661-0974, Japan; [c]HRI, AIST, 2217-14 Hayashi-cho, Takamatsu, Kagawa 761-0395, Japan; [d]Nanotube Research Center, AIST, Central 5, 1-1-1 Higashi, Tsukuba, Ibaraki 305-8565, Japan; [2]Present address: Department of Occupational Pneumology, Institute of Industrial Ecological Sciences, University of Occupational and Environmental Health, 1-1 Iseigaoka, Yahata-nishi-ku, Kitakyushu, Fukuoka 807-8555, Japan; [e]Department of Drug Delivery Research, Graduate School of Pharmaceutical Sciences, Kyoto University, 46-29 Yoshida Shimoadachi-cho, Sakyo-ku, Kyoto 606-8501, Japan; [f]Meijo University, 1-501 Shiogamaguchi, Tenpaku-ku, Nagoya 468-8502, Japan; and [g]NEC, 34 Miyukigaoka, Tsukuba, Ibaraki 305-8501, Japan

[1]To whom correspondence may be addressed. E-mail: e-miyako@aist.go.jp or iijimas@meijo-u.ac.jp.

SI Experimental Methods

Functional nanocarbon complexes. BSA–CNH complexes were prepared as follows. CNH (10 mg) (average diameter, about 80–100 nm; purity, 95%; metal-free) (supplied by NEC) and BSA (10 mg) (Wako) were sonicated for 30 min in medium (10 ml) on ice (<8°C) in an ultrasonication bath (USD-2R; power output, 80 W; oscillation frequency, 40 kHz; AS ONE) to obtain a uniform dispersion for subsequent *in vitro* and *in vivo* experiments. Fluorescent Alexa 488–BSA–CNH was obtained as follows. Carboxy-functionalized CNH (CNH–COOH) was prepared as described previously (1). The functional groups of CNH–COOH were estimated by the thermogravimetry-differential thermal analysis (TG-DTA) (TGA 2950; TA Instruments) (1). CNH–COOH (5 mg) and 1-ethyl-3-(3-dimethylaminopropyl) carbodiimide hydrochloride (WSC) (50 mg) (Wako) were sonicated in PBS (Wako) (pH 7.3, 5 ml) for 1 h. Temperature was maintained below 8°C using an ice bath. Alexa 488–BSA (5 mg) (Invitrogen) was dispersed in a black-coloured CNH–COOH aqueous solution (5 ml). After the mixture was vigorously stirred for 24 h at room temperature under shaded conditions, and was then filtered (Omnipore; pore size, 100 nm; Millipore) to remove the unreacted Alexa 488–BSA and washed with PBS (100 ml). Finally, Alexa 488–BSA–CNH complexes on a filter were resuspended in medium (10 ml) for subsequent *in vitro* experiments. Average particle size of Alexa 488–BSA–CNH complex was estimated about 150 nm by means of DLS analysis. Before the DLS measurement, The Alexa 488–BSA–CNH complex dispersion (5 μg/ml) was filtered though a cellulose acetate membrane (Advantec; pore size = 200 nm). Other BSA–functionalized CNTs, such as HiPco SWCNT [super-purified SWCNTs (purity, >95%); diameter, ~0.8–1.2 nm; length, ~0.1–1 μm; Unidym], CoMoCAT SWCNT [CG-100 (purity, >90%); diameter, ~0.7–1.3 nm; length, ~0.45–2.3 μm; SouthWest Nano Technologies] and MWCNT [purity, >95%; diameter, ~10–40 nm; length, ~10 μm; Meijo Nano Carbon], were prepared in a manner similar to BSA–CNH.

Characterisation of BSA–CNH. Sizes of BSA–CNH were measured using AFM (JSPM-4210; JEOL) (a tapping mode cantilever was used) and DLS (LB-550; HORIBA). The optical absorption spectra of BSA–CNH in several aqueous solutions were measured using an UV–vis–NIR spectrometer (V-630; JASCO) at room temperature.

Temperature assay. Dispersions of BSA–CNH (CNH concentration, 100 μg/ml) in cellular medium (250 μl) and cellular medium alone (as control) (250 μl) were irradiated with 670-nm laser light (spot diameter, ~5 mm) (BWF-670-300E; B&W Tek) at various power levels (50–300 mW). The temperature of the solutions (not directly under the laser beam) was measured using a K-type thermocouple probe (CT-280WR; Custom) or a temperature sensor (AD-5601A; A & D). Before experiments, the indicators for temperature measurements were calibrated to obtain accurate temperature values. Temperature elevations of various nanocarbon complex dispersions were investigated in a manner similar to those of BSA–CNH complex dispersions, except for the type of laser wavelength. The nanocarbon dispersions (250 μl) [nanocarbon concentration, 100 μg/ml; solvent, PBS buffer (pH 7.3)] were irradiated with continuous 785-nm laser light (spot diameter, ~4 mm) (BRM-785-1.0-100-0.22-SMA; B&W Tek) at 300 mW (~24 mW/mm^2) for 5 min. The temperatures of the dispersions were measured (not directly under the laser

beam) using the K-type thermocouple probe.

Plasmid construction. To construct reporter vectors, firefly luciferase *luc*2 of pHsp70-luc2 (gift from Dr H. Suzuki of Olympus) carrying the human Hsp70 promoter (2) (−193 to +1 bp, where +1 indicates the putative transcription start site) was replaced with *Hind*III and *Xba*I fragments of ELuc-PEST cDNA (Toyobo) of pSV40-dELuc (3) in which the PEST element of mouse ornithine decarboxylase was fused in frame to the C terminus of enhanced beetle luciferase ELuc (dELuc), resulting in pHsp70-dELuc. The Hsp70 promoer-dELuc-SV40 polyA cassette was PCR amplified using pHsp70-dELuc (template) and the following set of primers: 5′-GTACTAACATACGCTCTCCATC-3′ and 5′-GATGAGTTTGGACAAACCACAAC-3′. The amplified fragment product was digested with *Xba*I and ligated into a *Spe*I site upstream of IRES2 of pIRES2-AcGFP1 (Clontech) from which the cytomegalovirus (CMV) promoter was deleted by inverse PCR using a set of primers, 5′-ATGCATGGCGGTAATACGGTTATCCACAG-3′ and 5′-AGATACTAGTGCTCAAGCTTCGAATTCTGCAG-3′, resulting in pHsp70-dELuc-IRES-AcGFP1. To generate the pHsp70-DsRed vector, DsRed cDNA was PCR amplified using DsRed1-N1 (Clontech, template) and a set of primers, 5′-CCCAAGCTTCCACCATGGTGC-3′ and 5′-GCTCTAGACTACAGGAACAGGTG-3′, and digested with *Hind*III and *Xba*I. The product was ligated into the *Hind*III/*Xba*I fragment of pHsp70-luc2 from which luc2 cDNA had been removed.

Cell cultures and stable transfections. NIH 3T3 (RCB1826; RIKEN BioRecource Center), Colon-26 (RCB2657; RIKEN BioRecource Center) and C6 (JCRB9096; National Institute of Biomedical Innovation) cells were used for *in vitro* and *in vivo* experiments. The cells were typically seeded in 35-mm polystyrene dishes (Nunc) and grown in cell culture media supplemented with 10% FBS (JRH Biosciences) and an antibiotic mixture [penicillin (100 units/ml), streptomycin (100 μg/ml) and amphotericin B (250 ng/ml)] (antibiotic–antimycotic mixed stock solution; Nacalai). NIH 3T3 cells were grown in Dulbecco's Modified Eagle medium (DMEM) (Invitrogen). Colon-26 and C6 cells were grown in Roswell Park Memorial Institute 1640 (RPMI-1640) medium (Nacalai). For stable transfections, the reporter vector (pHsp70-dELuc-IRES-AcGFP1 or pHsp70-DsRed) and pcDNA3 (Invitrogen) were mixed at a ratio of 10:1 and introduced into cells using Lipofectamine 2000 (Invitrogen). Transfections with Lipofectamine 2000 were performed exactly as described in the manufacturer's manual. Stable transfected cell lines were constructed using the geneticin G418 sulphate (G418) resistance gene of cells. G418-resistant colonies were pooled and stable transfectants were maintained in medium supplemented with 10% FBS and the antibiotic mixture (above mentioned) containing G418 (500 μg/ml) (Nacalai). Using a fluorescent microscope (IX71; Olympus) and luminometer (AB-2250; Atto), expression of targeted proteins (GFP, DsRed and luciferase) in stable transfectants was confirmed after heating for 1 h at 37–50°C in a 5% CO_2 incubator (MCO-17AIC; Sanyo) or usual gas-phase incubator (MOV-212S; Sanyo) (Fig. S5).

Cellular uptake of CNH complexes. Cell densities in the media solutions were ~4×10^4 cells/cm^2. After incubation for 6 or 24 h at 37°C in 5% CO_2 atmosphere, cell culture media were replaced with the Alexa

488–BSA–CNH complex dispersion (5 μg/ml) consisting of 10% FBS, 25 mM 4-(2-hydroxyethyl)-1-piperazineethanesulfonic acid (HEPES)/NaOH (pH 7.0) and antibiotics, and cultures were incubated at 4 or 37°C. After incubation for 6 or 24 h, Alexa 488–BSA–CNH complex dispersions were removed and the cells were washed with fresh culture media. The cellular uptake of CNH complexes was investigated using a confocal microscope (FV10i; Olympus). The excitation wavelength was 488 nm, and fluorescence emission was detected at 525 nm.

Cytotoxicity tests of nanocarbon complexes. Mitochondrial enzyme activity was examined using WST-1. For the WST-1 assay, cells were seeded in 96-well plates (Nunc) at ~2×10^5 cells/well, incubated for 24 h, removed from the culture medium and then exposed to nanocarbon complex dispersions (100 μl/well) for 6 and 24 h. For the determination of mitochondrial enzyme activity, the cells were incubated with 10-fold diluted WST-1 solution (100 μl/well) (Premix WST-1 Cell Proliferation Assay System; Takara Bio) at 37°C for 2 h. The optical density of formazan was measured at 440 nm using a Multiskan Ascent plate reader (Thermo Labsystems). Measurements of intracellular caspase-3 activity were studied as follows. To obtain total cell extracts, nanocarbon complex-treated cells were collected with 0.25% trypsin, washed with cold PBS and resuspended for 10 min in ice-cold lysis buffer containing 150 mM NaCl, 50 mM Tris–HCl, pH 7.4, 50 mM NaF, 5 mM ethylenediaminetetraacetic acid (EDTA), 0.5% Triton X-100 and 1 mM Na_3VO_4, along with a protease inhibitor cocktail tablet (Roche Diagnostics GmbH). Nuclei and unlysed cell debris were removed by centrifugation at 10,000 *g* for 1 min. The protein concentration was determined using a BCA protein assay kit (Thermo Fisher Scientific), with BSA as a standard. Caspase-3 activity was measured by cleavage of the Asp-Glu-Val-Asp (DEVD) peptide-conjugated 7-amino-4-trifluoromethyl coumarin (AFC), according to the protocol outlined by the manufacturer of the caspase-3 fluorometric protease assay kit (Medical and Biological Laboratories). Substrate cleavage, which resulted in the release of AFC fluorescence (λ_{ex}, 400 nm; λ_{em}, 505 nm), was measured using a Fluoroskan Ascent CF plate reader. Cell death was determined using an apoptosis detection kit (Medical and Biological Laboratories). Treated cells were stained with annexin V-FITC and propidium iodide (PI) and analysed using a flow cytometer (Cytomics FC500 Flow Cytometry System; Beckman Coulter) equipped with a 488-nm argon laser. Data were collected for 10,000 events. Statistical analyses were performed using an analysis of variance with Tukey's test (ANOVA), and a p value of less than 0.05 was considered significant.

***In vitro* laser experiments.** Fluorescent proteins (GFP or DsRed) in cells were expressed using laser-induced CNH complexes as follows. The cells were irradiated in suspension for these experiments. The cells were seeded in 10-cm polystyrene dishes and grown in DMEM or RPMI-1640 media supplemented with 10% FBS, penicillin (100 units/ml), streptomycin (100 μg/ml), amphotericin B (250 ng/ml) and G418 (500 μg/ml). Cell densities in the media were ~4×10^4 cells/cm^2. After incubation for 24 h at 37°C in 5% CO_2 atmosphere, the culture medium was divided into four dispersions (250 μl × 4) of BSA–CNH (CNH concentration, 100 μg/ml). Obtained suspensions were added to poly(methyl methacrylate) (PMMA) cuvettes (Tokyo Glass Kikai) and irradiated with 670 and 785-nm laser light at various power levels [100 (~8 mW/mm^2) to 300 mW (~24 mW/mm^2)] for 30 min at room temperature.

After laser irradiation, the media were replaced with fresh media consisting of phenol red-free media (2 ml) containing 10% FBS, penicillin (100 units/ml), streptomycin (100 μg/ml), amphotericin B (250 ng/ml) and G418 (500 μg/ml). After overnight incubation, fluorescent protein expression in cells was investigated using the fluorescence microscope (IX71; Olympus) and analysed using analysis software (ImageJ; NIH). The laser-induced gene expression behaviour of the NIH 3T3 cells encapsulating BSA–CNH complexes were investigated as follows. Cell densities of NIH 3T3 in the media were ~4 × 10^4 cells/cm^2. After incubation for 24 h at 37°C in 5% CO_2 atmosphere, the culture medium was replaced with medium containing dispersed BSA–CNH (CNH concentration, 10 μg/ml). After incubation for 24 h at 37°C in 5% CO_2 atmosphere, the culture media were washed with cell medium to remove the extra CNH complexes, and then detached from the surface by the addition of trypsin-EDTA solution (Invitrogen) for laser radiation steps. Suspensions of the cells encapsulating CNH complexes (250 μL) were added to poly(methyl methacrylate) (PMMA) cuvettes and irradiated with 785-nm laser light at various power levels [50 (~4 mW/mm^2) to 500 mW (~40 mW/mm^2)] for 30 min at room temperature. After laser irradiation, the media were replaced with fresh media consisting of phenol red-free media (2 ml) containing 10% FBS, penicillin (100 units/ml), streptomycin (100 μg/ml), amphotericin B (250 ng/ml) and G418 (500 μg/ml). After overnight incubation, GFP expression in cells was investigated using the fluorescent microscope and analysed using analysis software.

Analysis of luciferase expression in NIH 3T3 cells was performed as follows. The cells were irradiated in monolayer for these experiments. NIH 3T3 cells were seeded in 35-mm glass-bottom dishes (Matsunami Glass Ind., Ltd.) and grown in DMEM medium supplemented with 10% FBS and antibiotics. Cell densities in the media were ~2 × 10^4 cells/cm^2. After incubation for 24 h at 37°C in 5% CO_2 atmosphere, the culture media in the dishes were replaced with media (250 μl) containing BSA–CNH (CNH concentration, 1000 μg/ml). After 670-nm laser irradiation for 30 min at room temperature, the media were replaced with fresh media consisting of phenol red-free DMEM (2 ml) containing 200 μM D-luciferin as a substrate (Toyobo), 10% FBS, 4 mM glutamine and 25 mM HEPES/NaOH (pH 7.0). Luciferase expression was monitored in real time using the luminometer.

Animal experiments. All animal experiments were performed strictly in accordance with protocols approved by the Institutional Animal Care and Use Committee of AIST and Kyoto University. Expression of Venus, a variant of yellow fluorescent protein, in transgenic medaka by laser-induced CNH was performed as follows. Transgenic medaka, transfected with olphsp70.1-hRluc-Venus, was prepared in a manner similar to that in our previous report (6). The 0.3% artificial seawater (250 μl) (Marin Art SF; Osaka Yakken) containing BSA–CNH (CNH concentration, 100 μg/ml) was added in PMMA cuvettes. Embryos or young transgenic medakas were added to the CNH dispersion. After 670-nm laser irradiation for 30 min, the dispersions were replaced with fresh 0.3% artificial seawater (250 μl) and incubated in polystyrene-type 96-well microplates (Nunc) overnight at 28°C. Medakas were not placed directly under the laser beam in an attempt to avoid phototoxic reactions. Venus expression in transgenic medaka was monitored using a fluorescence microscope (M205FA; Leica).

Luciferase was expressed by NIH 3T3 cells in a mouse as follows. Stable NIH 3T3 cell lines transfected

with pHsp70-dELuc-IRES-AcGFP1 were seeded in 10-cm polystyrene dishes (Nunc) and grown in DMEM media supplemented with 10% FBS and antibiotics. The cell density in the medium solution was ~4×10^4 cells/cm^2. After incubation for 24 h at 37°C in 5% CO_2 atmosphere, the culture media were replaced with media (100 μl) containing BSA–CNH (CNH concentration, 100 μg/ml). Suspensions of cells and BSA–CNH (50 μl) were injected at two positions on the back under the skin of a nude 8-week-old female mouse (n = 3; BALB/cSlc-nu/nu; Japan SLC). The injection site on one side was irradiated with 785-nm laser light for 30 min. During laser irradiation, temperature of the mouse's body surface was monitored by IR thermography (Ti10; Fluke), and the laser power was modulated to preset temperatures (39, 42 and 45°C). Laser power levels [~80–200 mW (~6–16 mW/mm^2)] had to be adjusted because pentobarbital anaesthesia caused significant temperature changes in the mouse. *In vivo* luciferase expression was monitored by bio-imaging (Nightowl NC320; Berthold Technologies), and picture processing was performed using ImageJ. Before imaging, D-luciferin solutions (6 mg/ml, 200 μl) (XenoLight Rediject D-Luciferin; Sumisho Pharma International) as substrates were injected into the abdominal cavity of the mouse.

CNH biocompatibility was investigated as follows. Saline (100 μl) containing BSA–CNH (CNH concentration, 100 μg/ml) or only saline (100 μl) was injected into the back under the skin of a 7-week-old female mouse (n = 5; BALB/cSlc; Japan SLC). After 7 and 30 days, blood samples were collected from the inferior vena cava of the mouse and the injected area was observed by incising an affected site (Fig. 4). Complete blood cell count (CBC) and biochemical examination were performed by BioGate Co., Ltd and Oriental Yeast Co., Ltd (Table 1). Pathological examinations of tissue slices were typically performed by Hist Science Laboratory Co., Ltd. In brief, after the test periods, animals were euthanised by exsanguination under pentobarbital anaesthesia, and their tissues were autopsied. Skin tissues were fixed in 10% buffered formalin, embedded in paraffin, sectioned, stained with hematoxylin and eosin (HE) and then histopathologically observed under an optical microscope. Immunohistochemical staining of macrophages was performed at Hist Science Laboratory Co., Ltd. In brief, sections were prepared from the paraffin blocks. The sections were deparaffinised in xylene and ethanol. After rinsing, endogenous peroxidase was blocked by incubation with 3% H_2O_2 for 5 min. The sections were then incubated overnight with Iba1 (1:400) (Wako) at room temperature. After rinsing, the sections were incubated with the secondary antibodies [Histofine Simple Stain Mouse MAX PO (Rat); Nichirei] for 30 min at room temperature. After washing, Iba1-specific immunolabelling was examined using diaminobenzidine (Nichirei). Nuclei were also stained with hematoxylin.

SI text

Characterisation of BSA–CNH complexes. Structural characterisation, photothermostability and cytotoxicity analyses of BSA–CNH complexes were investigated (Fig. S1). Average size of BSA–CNH was estimated about 100~200 nm by AFM and DLS (Figs. S1*A* and S1*B*). DLS is a powerful technique for the sizing of nanoparticles and characterization of their properties in the liquid phase (7). The BSA–CNH was highly stable in DMEM containing 10% FBS with no aggregation after 7 days in storage at 4°C (Figs. S1*C*). Average size of BSA–CNH remained about the same for 7 days. We observed no sedimentation of the

functionalised CNH complexes, even at a relatively high laser power (300 mW) (Fig. S1*D*). The temperature directly under the laser beam path could be significantly greater than the temperature outside of the path (Fig. S1*E*). We also investigated the effect of CNH concentration on the temperature increase (Fig. S1*F*). The optimal concentration of CNH for effective heating of solution was ca. 100 μg/ml. The BSA–CNH complex dispersion was applied to NIH 3T3, Colon-26 and C6 cells, and mitochondrial enzyme activities were measured after 6 and 24 h using the WST-1 assay (Fig. S1*G*). We consider that WST-1 assay is suitable for the evaluation of the cytotoxicity of nanocarbons (4, 5). In all cases, most cells were alive even when cells were exposed to highly concentrated CNH dispersions (1000 μg/ml). Next, intracellular caspase-3 activity was investigated as an apoptosis marker (Fig. S1*H*). No significant increases in caspase-3 activity were observed in any cell. Cell viability was also measured by flow cytometry (Fig. S1*I*). The cells exposed to BSA–CNH complex dispersions for 24 h were stained with annexin V-FITC and PI, and fluorescence was measured by flow cytometry. Most cells were normal. Both annexin V-FITC and PI fluorescence did not increase significantly. This result indicates that BSA–CNH does not dramatically induce apoptosis or necrosis in cultured cells following 24 h of exposure. These results definitively indicate that BSA–CNH has low cytotoxicity.

Dispersion property of BSA–nanocarbon complexes. Dispersion property of BSA–nanocarbon complexes was investigated (Fig. S2). BSA–CNH is well dispersed in PBS without visible aggregations even after incubation for 24 h. BSA–CNT is dispersed in PBS to some extent, with CNT aggregations being deposited at the bottoms of vials after incubation for 24 h. Most BSA–CNH complexes are suspended in a supernatant after centrifugation. In contrast, a large amount of CNTs are deposited at the bottoms of microtubes. These results clearly indicate that BSA molecules have greater dispersion ability for CNH than for CNTs.

Cellular uptake of CNH complexes. We synthesized the fluorescent Alexa 488–BSA–CNH complex by covalent technique to prevent the uptake of unattached Alexa 488–BSA molecules into cells (1, 8). When NIH 3T3 cells were incubated with Alexa 488–BSA–CNH complex dispersions at 37°C, cellular uptake was observed using a confocal microscope. The fluorescent image (Fig. S3*A Left*), the DIC image (Fig. S3*A Centre*), and a combination of the two images (Fig. S3*A Right*) revealed that fluorescence was mainly emitted from the cell interior, indicating that Alexa 488–BSA–CNH was taken inside the cells. To study the mechanism of cellular uptake of Alexa 488–BSA–CNH, we incubated the cells with cellular media containing Alexa 488–BSA–CNH at 4°C for 24 h. The confocal microscope images revealed (Fig. S3*B*) that Alexa 488–BSA–CNH was located mainly around the cell membranes but not inside the cells, indicating that cell internalisation was energy dependent. Thus, endocytosis (1, 8) is a possible cellular uptake pathway for these nanostructures. In other cells (Colon-26 and C6), we also confirmed an endocytotic phenomena associated with Alexa 488–BSA–CNH (Figs. S3*E–L*). In addition, uptake of Alexa 488–BSA–CNHs into cells was slow although Alexa 488–BSA–CNH was absorbed onto the cell surfaces when the cells were incubated at 37 or 4°C for short-time exposure treatment (6 h).

Protein expression in cells triggered by laser-induced CNH complexes. Protein expression behaviour in cells was observed after laser irradiation or incubation in thermostatic chambers (Figs. S4–S6). The optimal laser powers for effective gene expression in cells were determined (Fig. S4). We confirmed that the distinguished NIH 3T3 cell death did not occur under the optimal laser power (Fig. S4*C*). In addition, influence of temperature on protein expression in cells was investigated (Fig. S5). When the incubation temperature was 42°C, NIH 3T3 cells effectively expressed a large amount of GFP and luciferase (Fig. S5*A–F*). In addition, GFP expression behaviour is the same in both adherent and floating cell systems. Furthermore, when the preset temperature was 42°C, maximum fluorescent protein expression levels were obtained in other cells (Colon-26 and C6) (Fig. S5*G–P*). We confirmed that these cells were destroyed by treatment with high temperature (over 45°C). In addition, NIH 3T3 cell death was also observed by the excess photothermal properties of CNH complexes (Fig. S6). These results indicated that the optimal temperature for effective gene expression was approximately 42°C. We have investigated the laser-induced gene expression behaviour of the NIH 3T3 cells encapsulating BSA–CNH complexes in order to reduce the amount of CNHs administered (Fig. S7). Maximum GFP expression was observed at 300 mW (~24 mW/mm^2). We also observed that high power laser irradiation (> 350 mW) damages cells.

Repeatability tests. We obtained almost the same results and confirmed the reproducibility (Fig. S8).

Laser-irradiated areas. Burn injury appeared near the injected areas only at 45°C (Fig. S9).

1. Zhang M, Yudasaka M, Ajima K, Miyawaki J, Iijima S (2007) Light-assisted oxidation of single-wall carbon nanohorns for abundant creation of oxygenated groups that enable chemical modifications with proteins to enhance biocompatibility. *ACS Nano.* 1:265–272.
2. Wu BJ, Kingston RE, Morimoto RJ (1986) Human HSP70 promoter contains at least two distinct regulatory domains. *Proc. Natl. Acad. Sci. USA* 83:629–633.
3. Nakajima Y, *et al*. (2010) Enhanced beetle luciferase for high-resolution bioluminescence imaging. *PLoS One* 5:e10011.
4. Horie M, Kato H, Fujita K, Endoh S, Iwahashi H, (2011) *In vitro* evaluation of cellular response induced by manufactured nanoparticles. *Chem. Res. Toxicol.* doi:10.1021/tx200470e.
5. Wörle-Knirsch JM, Pulskamp K, Krug HF, (2006) Oops they did it again! carbon nanotubes hoax scientists in viability assays. *Nano Lett.* 6:1261–1268.
6. Oda S, *et al*. (2010) Identification of a functional medaka heat shock promoter and characterization of its ability to induce exogenous gene expression in medaka *in vitro* and *in vivo*. *Zoolog. Sci.* 27:410–415.
7. Takahashi K, Kato H, Saito T, Matsuyama S, Kinugasa S, (2008) Precise measurement of the size of nanoparticles by dynamic light scattering with uncertainty analysis. *Part. Part. Syst. Char.* 25:31–38.
8. Silverstein SC, Steinman RM, Cohn ZA. (1977) Endocytosis. *Annu. Rev. Biochem.* 46:669–722.

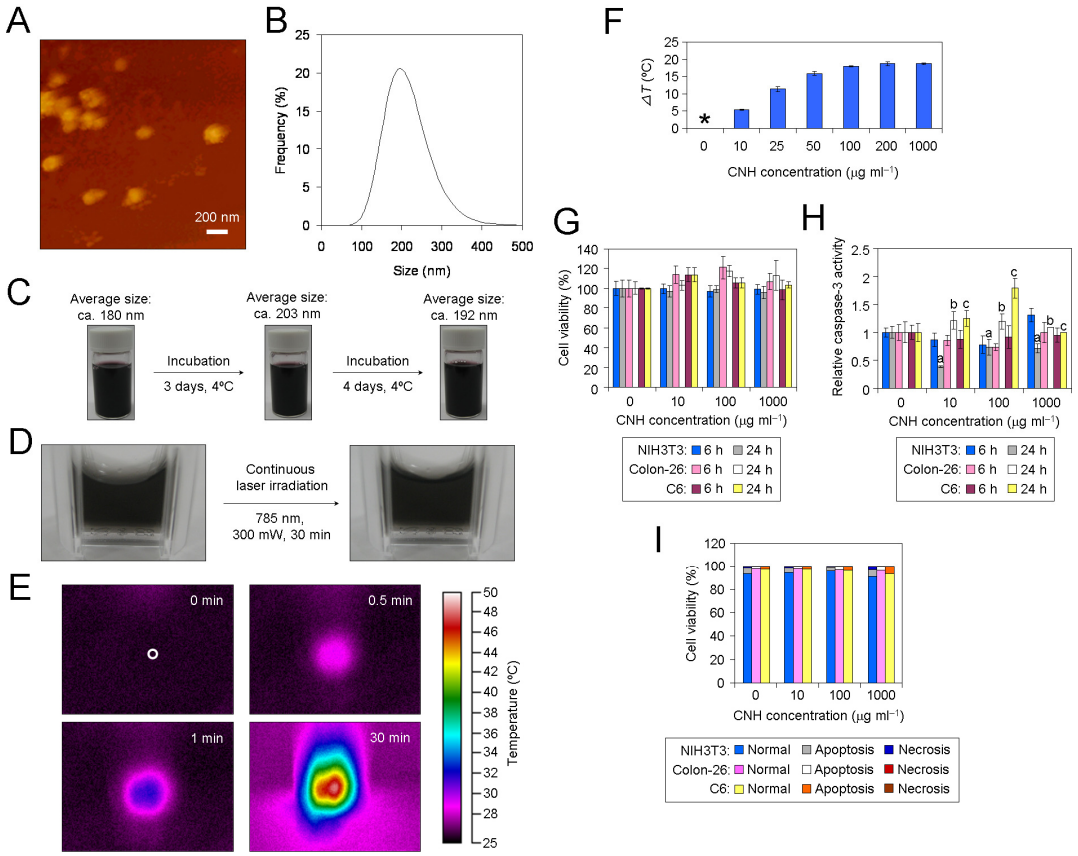

Fig. S1. Characterisation of BSA–CNH complexes. (*A–C*) Structural characterisation and photothermostability of BSA–CNH complexes. (*A*) AFM image of BSA–CNH complexes. (*B*) DLS analysis of BSA–CNH. (*C*) Photos of BSA–CNH dispersions in DMEM containing 10% FBS after incubation at 4ºC for 7 days. The concentration of CNH was 100 μg/ml. Average sizes of CNH complexes were measured by DLS. (*D*) Photographs of 0.01 wt% BSA–CNH in 0.3% artificial seawater after 785-nm laser irradiation for 30 min. Laser power = 300 mW (~24 mW/mm^2). (*E*) Thermographic measurement of 0.01 wt% BSA–CNH in DMEM containing 10% FBS after 785-nm laser irradiation for 30 min. White circle indicates the laser spot. (*F*) Photoinduced temperature elevation at various CNH concentrations under continuous 785-nm laser irradiation at 300 mW (~24 mW/mm^2) for 5 min. * = Not determined because the temperature did not increase. (*G–I*) Cytotoxicity analyses of BSA–CNH complexes. (*G*) Effect of BSA–CNH complexes on mitochondrial enzyme activity determined by a 2-(4-iodophenyl)-3-(4-nitrophenyl)-5-(2,4-disulfophenyl)-2H-tetrazolium monosodium salt (WST-1) assay. The percentage of mitochondrial enzyme activity compared with the standardised control was 100%. NIH 3T3, Colon-26 and C6 cells were exposed to the BSA–CNH complex dispersion at various concentrations for 6 and 24 h. (*H*) Caspase-3 activity in cells exposed to BSA–CNH. The value of activity in the standardised untreated cells was set to 1. Statistical analysis was carried out using ANOVA (Tukey's test). $^{a}p < 0.05$, $^{b}p < 0.0001$; $^{c}p < 0.0025$. (*I*) Detection of apoptotic cells following BSA–CNH exposure. The data are presented as the percentage of apoptotic cells among 10,000 cells. Values are averages of three independent experiments. An index of living cells is a well-established measure of mitochondrial enzyme activity.

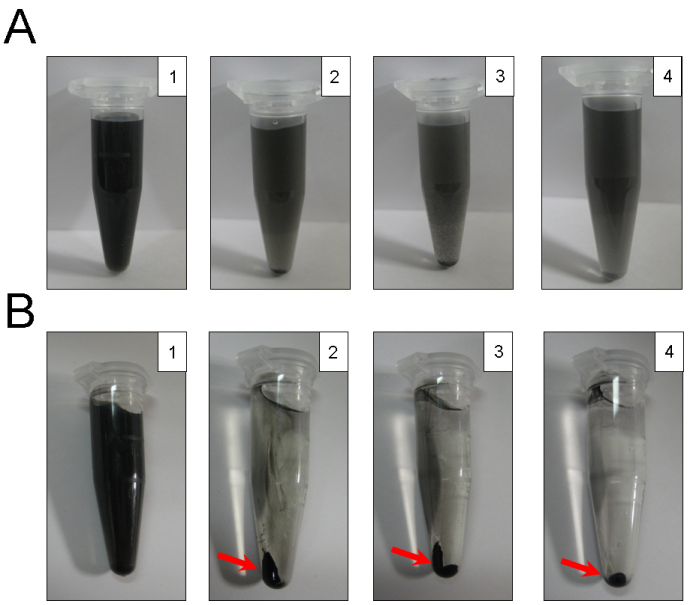

Fig. S2. Dispersion property of BSA–nanocarbon complexes. (*A*) Photos of BSA-functionalised nanocarbon complexes in PBS after immediate ultrasonication. (*B*) Photos of nanocarbon complexes after centrifugation (9100 *g*, 15 min, 4°C). Red arrows indicate the precipitates derived from CNT aggregations. (1) CNH, (2) high-pressure carbon monoxide (HiPco) SWCNT, (3) cobalt–molybdenum catalyst (CoMoCAT) SWCNT and (4) MWCNT. Concentrations of nanocarbons are 100 μg/ml.

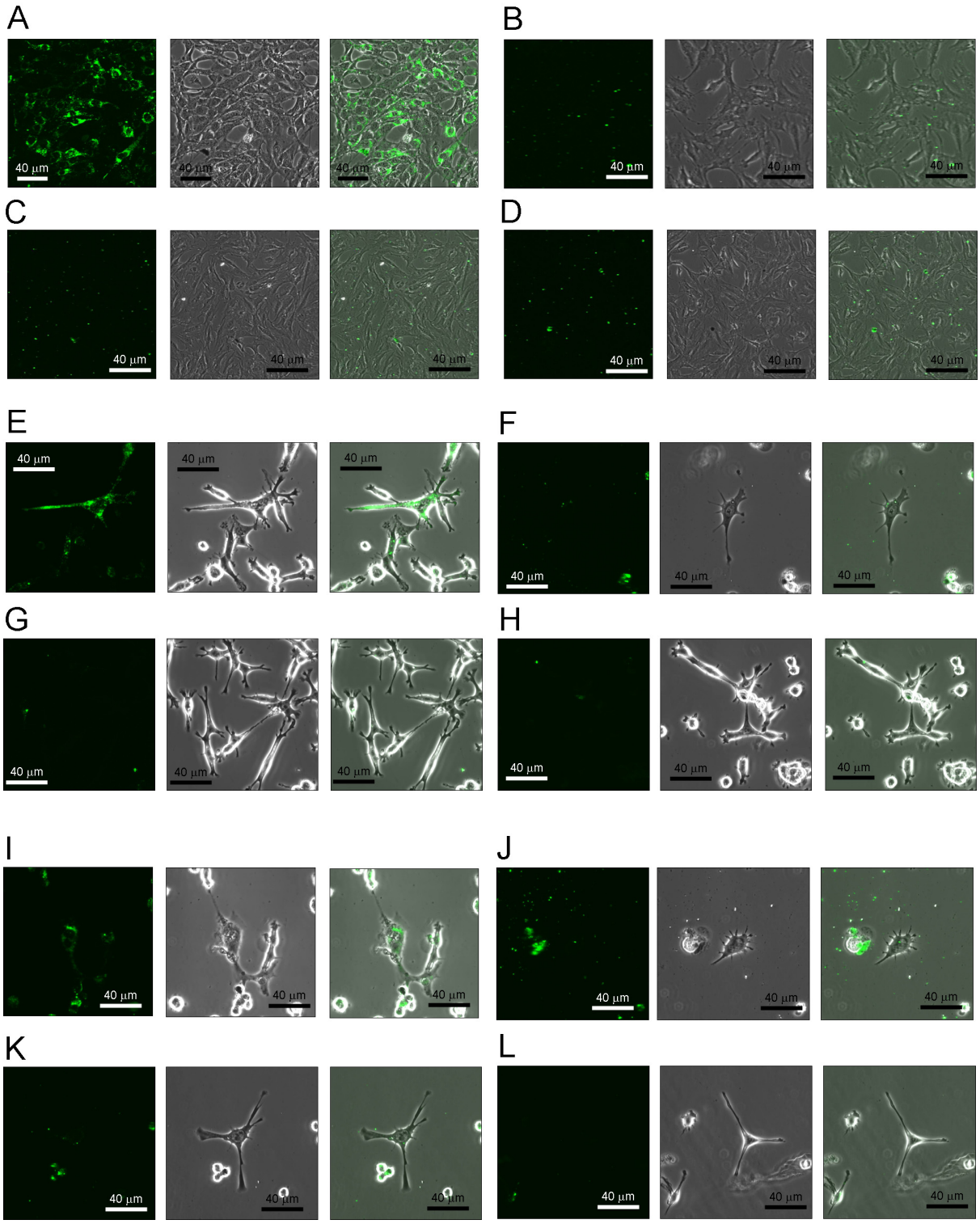

Fig. S3. Confocal microscopy images of various cells after incubation with Alexa 488–BSA–CNH complexes. (*A–D*) NIH 3T3, (*E–H*) Colon-26 and (*I–L*) C6 cells. (*A–L*) Fluorescence (left), differential interference (DIC) contrast (centre) and a combination of fluorescence and DIC images (right). (*A*, *E*, *I*) Incubation time = 24 h, Incubation temperature = 37°C. (*B*, *F*, *J*) Incubation time = 24 h, Incubation temperature = 4°C. (*C*, *G*, *K*) Incubation time = 6 h, Incubation temperature = 37°C. (*D*, *H*, *L*) Incubation time = 6 h, Incubation temperature = 4°C.

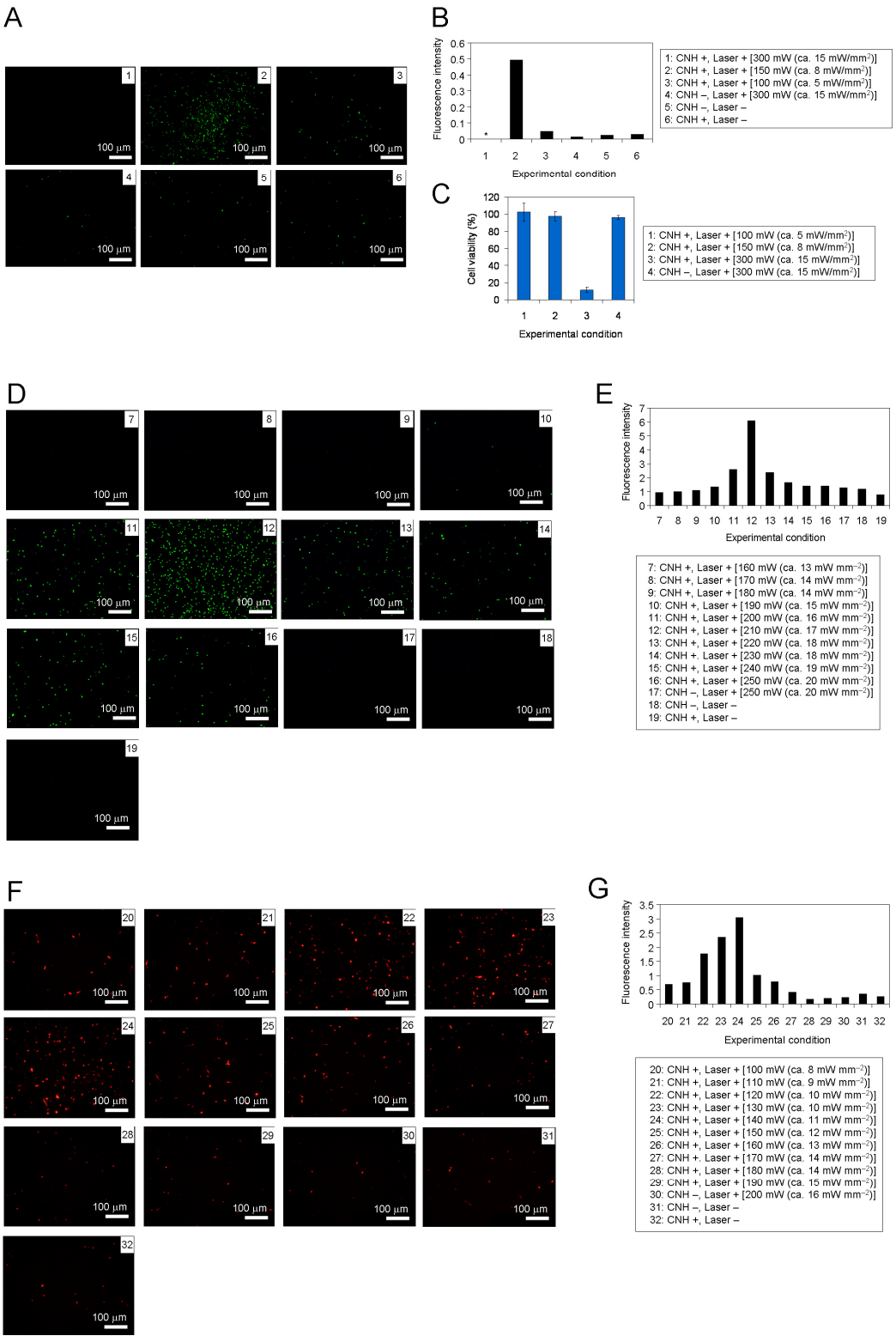

Fig. S4. Protein expression in cells triggered by laser-induced CNH complexes. (*A* and *B*) GFP expression in stably transfected NIH 3T3 cells triggered by 670-nm laser-induced CNH complexes. * = Not determined because no fluorescence was detected. (C) WST-1 assay of NIH 3T3 cells after laser-induced CNH complexes. (*D* and *E*) GFP expression in stably transfected Colon-26 cells triggered by 785-nm laser-induced CNH complexes. (*F* and *G*) DsRed expression in stably transfected C6 cells triggered by 785-nm laser-induced CNH.

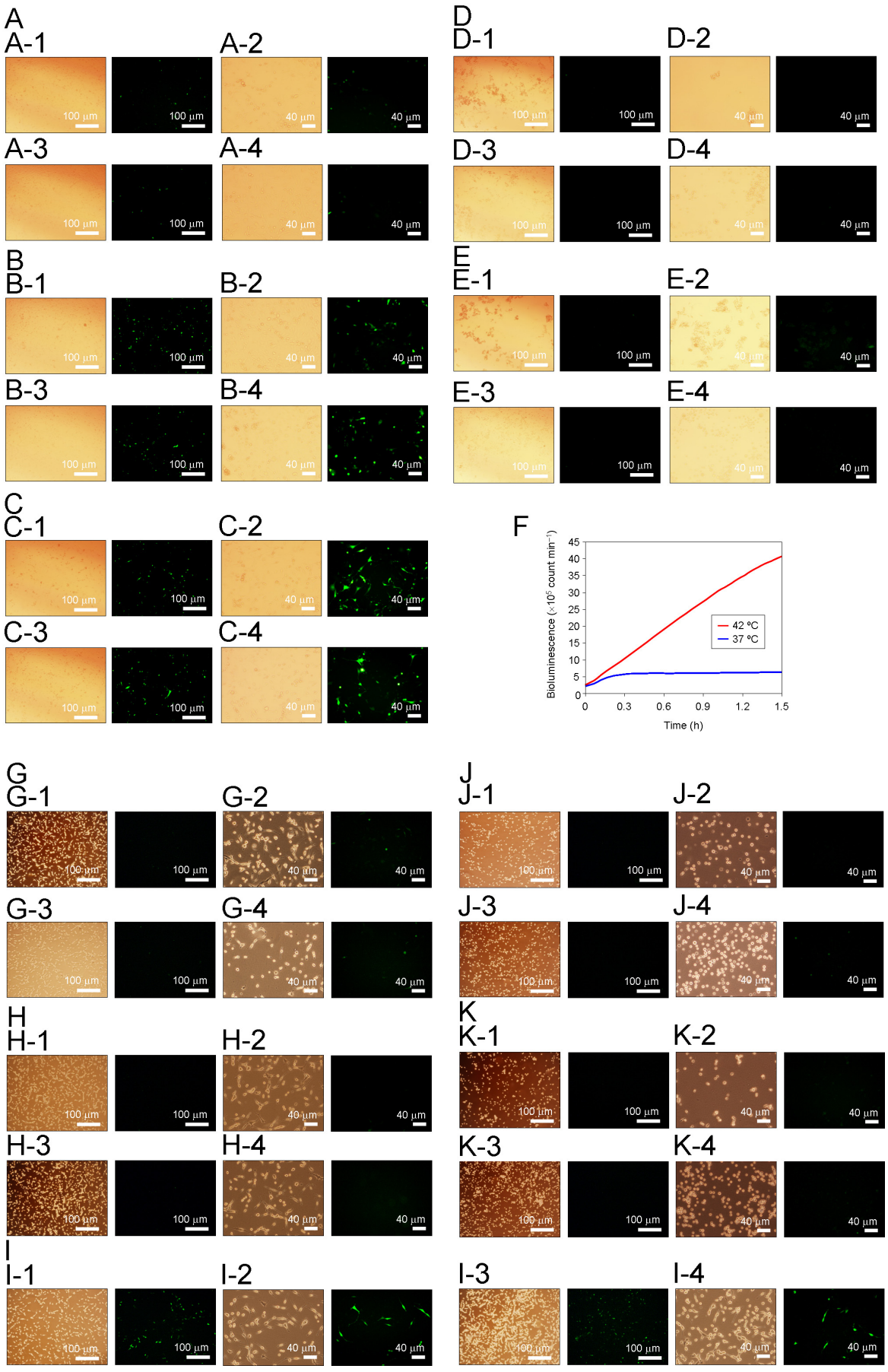
A
A-1
A-2
A-3
A-4
B
B-1
B-2
B-3
B-4
C
C-1
C-2
C-3
C-4
D
D-1
D-2
D-3
D-4
E
E-1
E-2
E-3
E-4
F
Bioluminescence (×10⁵ count min⁻¹)
Time (h)
42 °C
37 °C
G
G-1
G-2
G-3
G-4
H
H-1
H-2
H-3
H-4
I
I-1
I-2
I-3
I-4
J
J-1
J-2
J-3
J-4
K
K-1
K-2
K-3
K-4
100 μm
40 μm

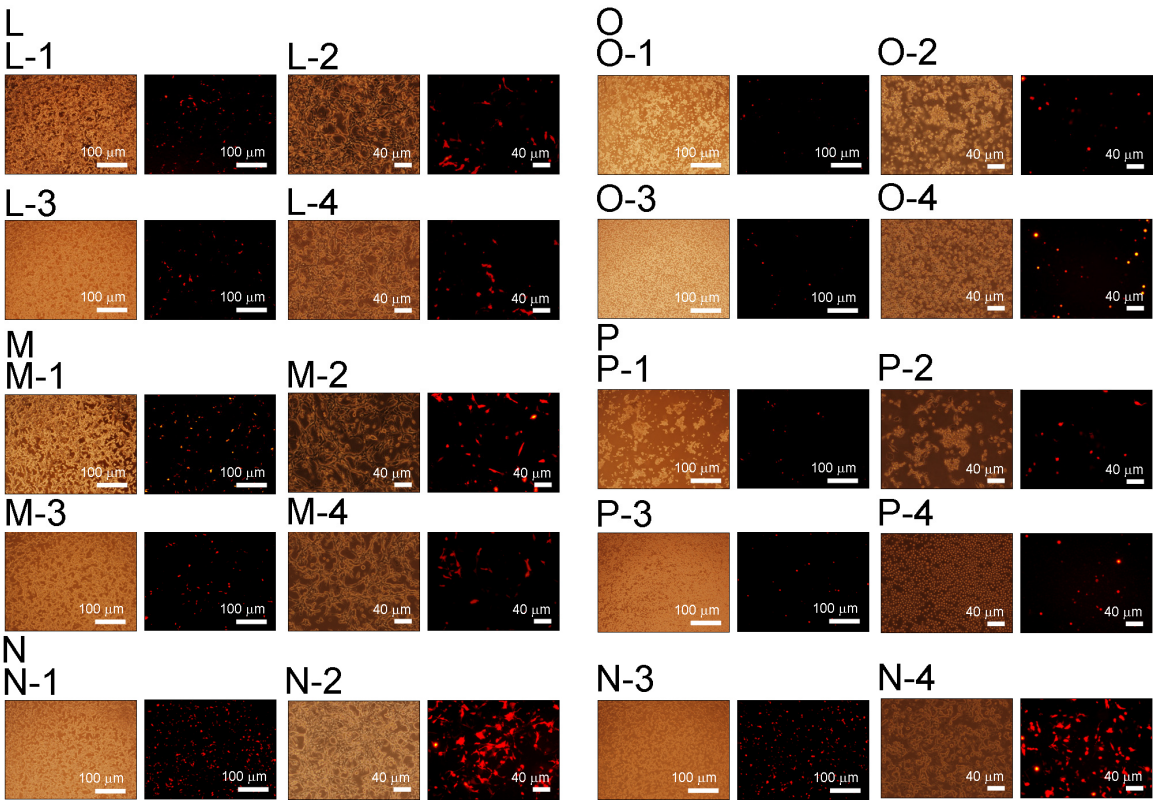

Fig. S5. Influence of temperature on protein expression in cells. (*A–F*) Influence of temperature on GFP and luciferase expression in stably transfected NIH 3T3 cells. (*A–D*) Fluorescent microscopy images of NIH 3T3 cells after heating for 1 h at various temperatures (37, 40, 42, 45 and 50°C). (*F*) Influence of temperature on luciferase expression in NIH 3T3 cells. (*G–K*) Influence of temperature on GFP expression in stably transfected Colon-26 cells. (*L–P*) Influence of temperature on DsRed expression in stably transfected C6 cells. (*A, G, L*) Incubation temperature = 37°C. (*B, H, M*) Incubation temperature = 40°C. (*C, I, N*). Incubation temperature = 42°C. (*D, J, O*) Incubation temperature = 45°C. (*E, K, P*) Incubation temperature = 50°C. Low magnification (×4) images of adherent [*X*−1 (*X* = *A–P*)] and floating [*X*−3 (*X* = *A–P*)] cell systems. High magnification (×10) images of adherent [*X*−2 (*X* = *A–P*)] and floating [*X*−4 (*X* = *A–P*)] cell systems. DIC (left) and fluorescence (right) images.

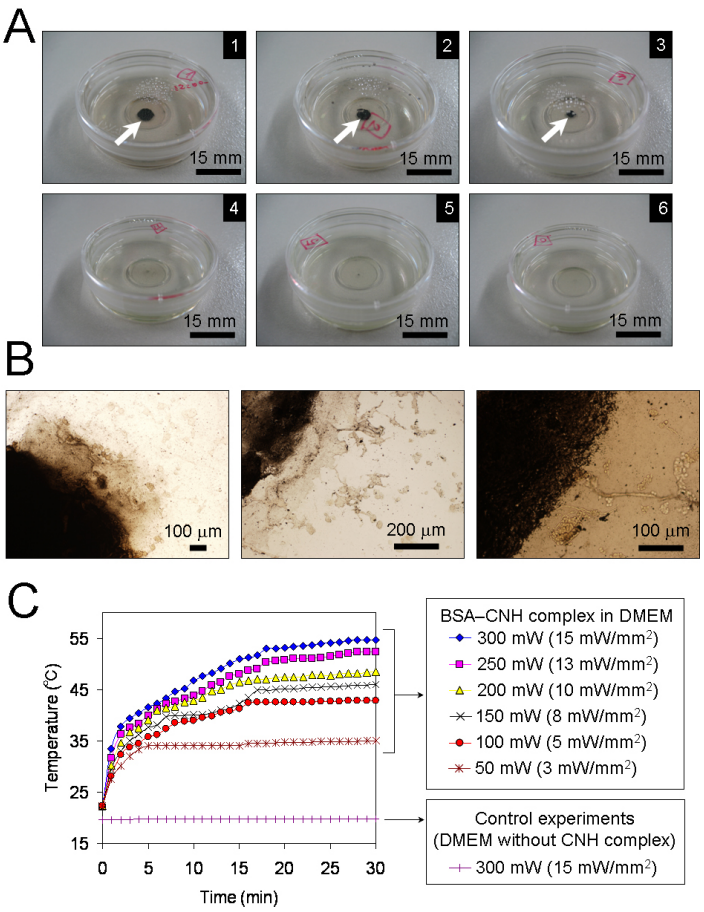

Fig. S6. Observation of NIH 3T3 cell death driven by the photothermal properties of CNH complexes. (*A*) Photographs of cell dishes after laser irradiation [(1) 300 mW (~15 mW/mm^2), (2) 250 mW (~13 mW/mm^2), (3) 200 mW (~10 mW/mm^2), (4) 150 mW (~8 mW/mm^2), (5) 100 mW (~5 mW/mm^2) and (6) 50 mW (~3 mW/mm^2)]. (*B*) Optical microscopy images of NIH 3T3 cell death at various objective magnifications (left: ×4, centre: ×10, right: ×20). (*C*) Increases in the temperature of BSA–CNH complex dispersions (250 μl, CNH concentration = 1000 μg/ml) in glass bottom dishes under continuous 670-nm laser irradiation at various laser powers [50 mW (~3 mW/mm^2)–300 mW (~15 mW/mm^2)]. We used a high concentration of CNH sample (1000 μg/ml) in this experiment for effective heating of the solution in a large-sized dish (35 mm).

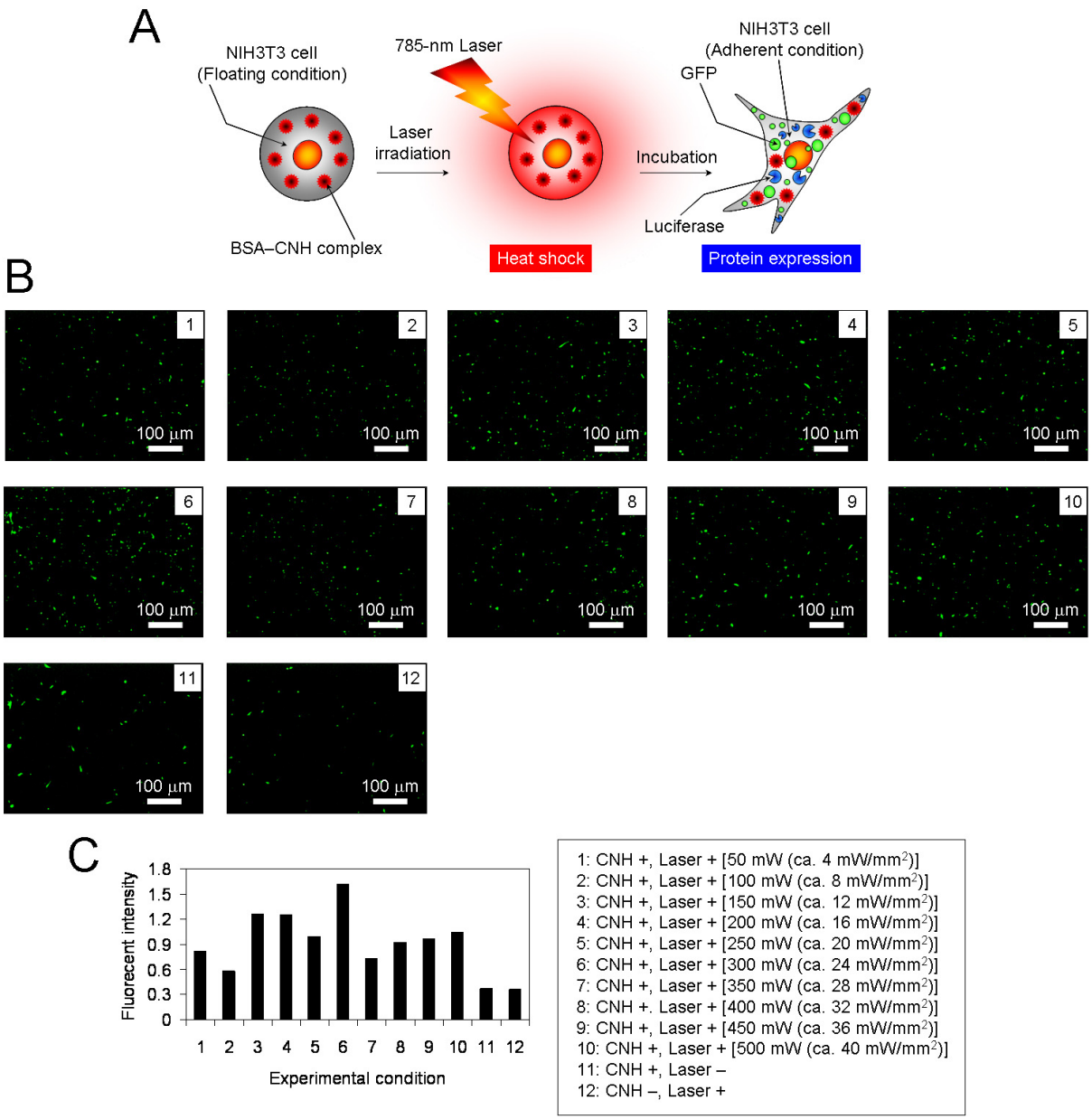

Fig. S7. (*A*) Schematic illustration of this experiment. (*B* and *C*) GFP expression behaviour of the laser-induced NIH 3T3 cells encapsulating BSA–CNH complexes triggered by 785-nm laser-irradiation.

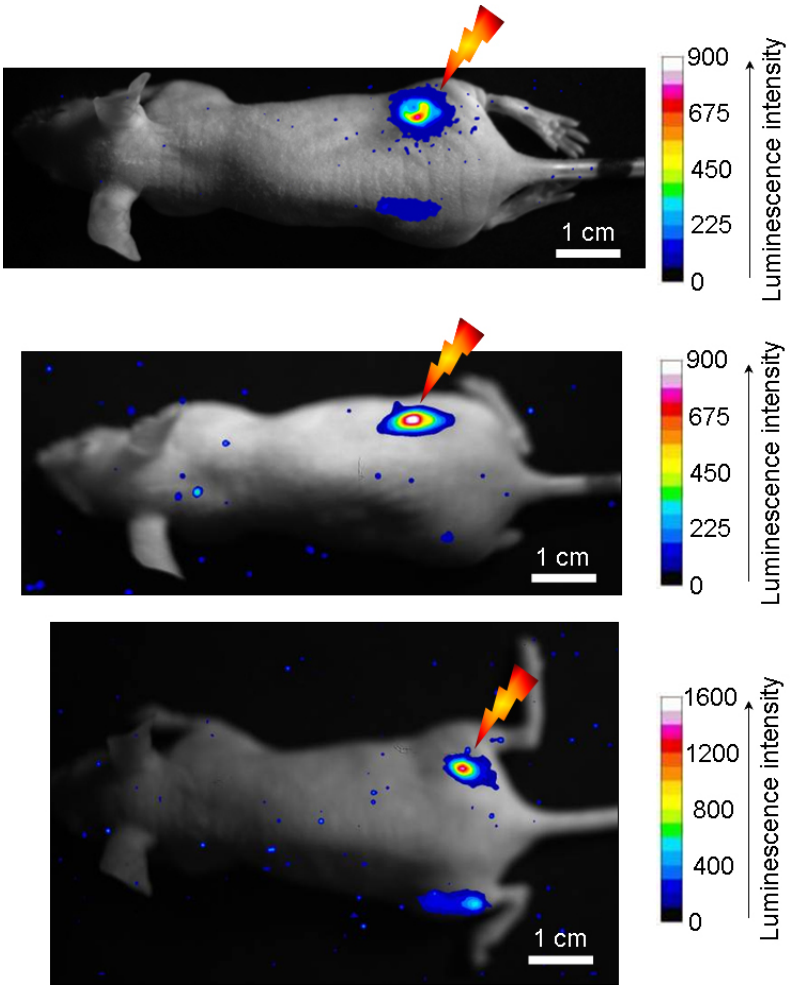

Fig. S8. Luciferase expression in stably transfected NIH 3T3 cells injected under the skin of three different nude mice after 785-nm laser irradiation. Preset temperature = 42°C.

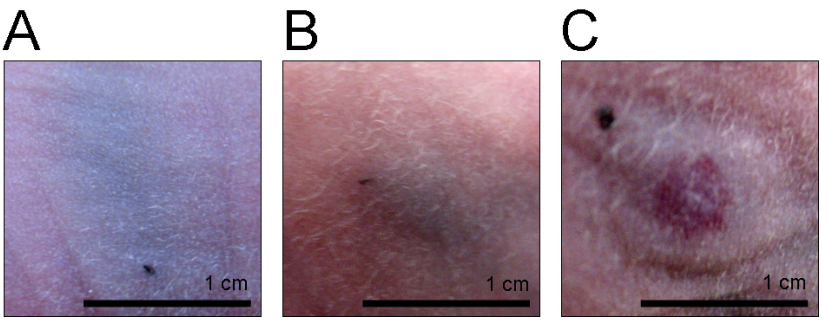

Fig. S9. Photographs of laser-irradiated areas. Preset temperatures: (i) 39°C, (ii) 42°C and (iii) 45°C.